Earth's Future

Key Points:
- Precipitation events are projected to become larger and the duration between these events will be longer
- Heavily managed river basins in the northern and midlatitudes will experience considerable hydrological intensification
- Water infrastructure and management will likely be challenged to balance flood protection and water supply among competing water uses

Supporting Information:

Supporting Information may be found in the online version of this article.

Author Contributions:
Conceptualization: Darren L. Ficklin, Sarah E. Null, John T. Abatzoglou, Kimberly A. Novick
Formal analysis: Darren L. Ficklin, Sarah E. Null, Daniel T. Myers
Methodology: Darren L. Ficklin, Sarah E. Null, John T. Abatzoglou, Kimberly A. Novick

Hydrological Intensification Will Increase the Complexity of Water Resource Management

Darren L. Ficklin[1] , **Sarah E. Null[2]** , **John T. Abatzoglou[3]** , **Kimberly A. Novick[4]** , and **Daniel T. Myers[1]**

[1]Department of Geography, Indiana University, Bloomington, IN, USA, [2]Department of Watershed Sciences, Utah State University, Logan, UT, USA, [3]Management of Complex Systems, University of California, Merced, CA, USA, [4]O'Neill School of Public and Environmental Affairs, Indiana University, Bloomington, IN, USA

Abstract Global warming intensifies the hydrological cycle by altering the rate of water fluxes to and from the terrestrial surface, resulting in an increase in extreme precipitation events and longer dry spells. Prior hydrological intensification work has largely focused on precipitation without joint consideration of evaporative demand changes and how plants respond to these changes. Informed by state-of-the-art climate models, we examine projected changes in hydrological intensification and its role in complicating water resources management using a framework that accounts for precipitation surplus and evaporative demand. Using a metric that combines the difference between daily precipitation and daily evaporative demand (surplus events) and consecutive days when evaporative demand exceeds precipitation (deficit time), we show that, globally, surplus events will become larger (+11.5% and +18.5% for moderate and high emission scenarios, respectively) and the duration between them longer (+5.1%; +9.6%) by the end of the century, with the largest changes in the northern latitudes. The intra-annual occurrence of these extremes will stress existing water management infrastructure in major river basins, where over one third of years during 2070–2100 under a moderate emissions scenario will be hydrologically intense (large intra-annual increases in surplus intensity and deficit time), tripling that of the historical baseline. Larger increases in hydrologically intense years are found in basins with large reservoir capacity (e.g., Amazon, Congo, and Danube River Basins), which have significant populations, irrigate considerable farmland, and support threatened and endangered aquatic species. Incorporating flexibility into water resource infrastructure and management will be paramount with continued hydrological intensification.

Plain Language Summary Climate change is intensifying the hydrologic cycle, resulting in an increase in floods and droughts. These changes increase the complexity of water resource management that must balance between releasing water to reduce flood risk and storing water for long periods without precipitation. Using updated climate model projections, we show that the amount of precipitation during events will become larger combined with longer dry periods where the daily evaporative demand exceeds precipitation for much of the Earth's surface. Additionally, for the late 21st century, a large portion of the years will be hydrologically intense in major river basins, resulting in conditions that deviate from those for which infrastructure and management policies were developed.

1. Introduction

Increasing air temperatures lead to an intensification of the global hydrologic cycle, defined here as an increase in fluxes of water between the atmosphere and terrestrial surface. Warming increases the saturation vapor pressure of air, potentially leading to an increase in both precipitation and evaporative demand (Allen & Ingram, 2002; Ficklin & Novick, 2017). The Clausius-Clapeyron relationship suggests an increase in water vapor by approximately 6%–7%/°C; however, when constrained by the energy balance, atmospheric water vapor may only increase ~2%–3%/°C (Allan et al., 2020; Allen & Ingram, 2002; Trenberth et al., 2003). Even so, hydrological intensification results in more extreme precipitation events (Kirchmeier-Young & Zhang, 2020; Pendergrass & Knutti, 2018; Polson et al., 2013) and disproportionately increases the magnitude of precipitation extremes relative to total annual precipitation (Donat et al., 2013; O'Gorman, 2015; Pendergrass & Knutti, 2018; Polade et al., 2014). These shifts in the distribution imply a concurrent increase in the frequency and/or duration of dry events (He & Sheffield, 2020; Polade et al., 2014; Wainwright et al., 2021) facilitating projected increases in the frequency and severity of drought for some regions (Cook et al., 2020).

Visualization: Darren L. Ficklin, Sarah E. Null, John T. Abatzoglou, Kimberly A. Novick, Daniel T. Myers
Writing – original draft: Darren L. Ficklin, Sarah E. Null, John T. Abatzoglou, Kimberly A. Novick
Writing – review & editing: Darren L. Ficklin, Sarah E. Null, John T. Abatzoglou, Kimberly A. Novick, Daniel T. Myers

However, most efforts to quantify hydrological intensification have focused solely on precipitation changes (Huntington et al., 2018), which do not capture the role of rising atmospheric demand. Increasing evaporative demand (which is often described in terms of a reference, well-watered evapotranspiration rate, or ETo) is an important signal of hydrological intensification, as greater ETo dries out soil more quickly after precipitation events (Ficklin et al., 2019; Huntington et al., 2018). Actual evapotranspiration is also likely to increase as ETo rises, at least initially in places not water-limited. Increases in actual and reference/potential evapotranspiration rates have been observed (Greve et al., 2014; Greve & Seneviratne, 2015; Huntington et al., 2018; Milly & Dunne, 2016) and are projected to continue with climate change (Ficklin et al., 2019; Lavers et al., 2015; McEvoy et al., 2020). However, eventually, plants close their stomata directly in response to the increases in vapor pressure deficit (VPD) that accompany increasing ETo (Grossiord et al., 2020), which decouple actual evapotranspiration from its reference rate (Novick et al., 2016). The increases in atmospheric CO_2 can also independently reduce stomatal conductance (Ainsworth et al., 2007; Swann et al., 2016) and further decouple actual and reference evapotranspiration. Therefore, a more integrated and robust signal of hydrological intensification should consider changes in both precipitation and changes in evaporative demand driven by rising temperature but mediated by dynamic plant responses to elevated VPD and CO_2. Prior work has characterized historical hydrological intensification based on changes in precipitation and actual evapotranspiration (Huntington et al., 2018). Future hydrological intensification has also been characterized based on changes in precipitation and reference evapotranspiration (Ficklin et al., 2019). Here, we build on the latter by describing and interpreting a novel metric to predict future hydrological intensification that treats plants as dynamic participants in the water cycle by accounting for plant stomatal closure as VPD and CO_2 increase.

Future changes to precipitation surplus and dry spell length that characterize hydrological intensification have important ramifications for a number of important societal problems. For example, not only periods of drought, but also periods of excess precipitation, can reduce agroecosystem productivity or alter the relationship between rainfall and plant growth (Felton et al., 2021; Post & King, 2020; Yin et al., 2020). Shifts in the distribution of rainfall events and dry spells have also been shown to influence landslide risk (Tichavský et al., 2019) and water quality (Loecke et al., 2017). Likely implications of increasing precipitation extremes and dry spells on water resource management are additional knowledge gaps that are directly confronted in this paper. Understanding which regions and river basins are anticipated to have larger precipitation events and longer dry spells is critical for designing and managing infrastructure for people, agriculture, and ecosystems. More frequent and severe floods and droughts are anticipated with climate change in some regions—including events that occur within the same year (Swain et al., 2018). These hydrologically intense years lead to increasing conflict among urban, agricultural, and ecological water uses, with intractable decisions for water resources managers about releasing water to alleviate flooding or storing water to meet demands later in the year (Raymond et al., 2020). Reservoir storage, conveyance, and flood control provide infrastructure to manage water resources with hydrological intensification, but paradoxically may also increase water demand because water is readily available, leaving communities that depend heavily on water infrastructure more vulnerable to hydrological intensification (Di Baldassarre et al., 2018).

Our overall objectives are twofold: (a) Understand projected changes in hydrological intensification that explicitly consider changes in precipitation, atmospheric demand, and dynamic plant feedbacks to rising atmospheric demand and elevated CO_2, and (b) relate patterns of future hydrological intensification to conflicting objectives for water resources management in major river basins throughout the world. Our approach relies on projections from an ensemble of climate models from the latest coupled model intercomparison project, CMIP6 (Eyring et al., 2016), and two Shared Socioeconomic Pathways (SSPs) SSP2-4.5 and SSP4-8.5 (O'Neill et al., 2016). While our previous work explored hydrological intensification for the continental United States using CMIP5 models (finding that including atmospheric demand rather than solely using precipitation resulted in increased intensification; Ficklin et al., 2019), global hydrological intensification has yet to be explored in detail using CMIP6 models. Additionally, we use descriptive information on human activities and important aquatic species occurring within river basins with considerable water storage to assess the influence hydrological intensification may have on water resource management. Quantifying hydrological intensification will improve understanding of the changing dynamics of water fluxes to and from the terrestrial surface for individual major river basins around the globe, therefore providing additional information on hydrological extremes and future water resource reliability.

2. Methods

2.1. Defining Hydrological Intensification

Here, hydrological intensification is defined as the annual average of daily precipitation surplus intensity (precipitation – ETo; in millimeters) and the annual average deficit time (specifically, the consecutive number of days when daily ETo > daily precipitation; Ficklin et al., 2019). By using both supply and atmospheric demand, our definition of hydrological intensification assesses how fast the water cycle is accelerating, considering both changes in extreme precipitation and the frequency of dry spells (Ficklin et al., 2019). Thus, our framework jointly considers how the variability in precipitation and atmospheric demand determines the patterns of hydrological intensification. Additionally, previous work has not included the direct consideration of the ways that plants respond to rising VPD and/or elevated CO_2 (Ficklin & Novick, 2017; Grossiord et al., 2020; Novick et al., 2016; Swann et al., 2016; Yuan et al., 2019). In other words, like many metrics to describe drought status and/or the pace of hydrological intensification, most prior work treats plants as static participants in the hydrologic cycle. Thus, a major novelty of the present study is its explicit consideration of dynamic plant response to VPD and CO_2.

The ETo was estimated using the American Society of Civil Engineers Penman-Monteith method for a reference grass surface, but with a formulation for the reference surface conductance that accounts for the influence of climate feedbacks on stomatal conductance, including rising CO_2 and VPD (Yang et al., 2019; see Supporting Information for details). These mechanisms reduce the magnitude of ETo, and failure to account for their influence on stomatal conductance can lead to overestimation of future ETo. Because we used an improved ETo model that includes the influence of CO_2 and VPD on stomatal conductance, our ETo is not directly comparable with ETo models that do not include this advancement. At the same time, this formulation does not explicitly consider soil moisture limitations to stomatal function, and thus the ETo should not be interpreted as actual evapotranspiration; rather, it should be interpreted as the ETo rate for conditions of non-limiting soil moisture, but with the potential for VPD and CO_2 to reduce stomatal conductance. While declining soil moisture may cause additional reductions to the actual ET, VPD and soil moisture are coupled in time and space (Zhou et al., 2019), and VPD is the predominant factor limiting transpiration in many parts of the world (Flo et al., 2021; Novick et al., 2016).

We used a metric for hydrological intensification that blends information about surplus intensity and deficit time—the Surplus Deficit Intensity Index (or SDI; Equation 1; Ficklin et al., 2019) defined as:

$$SDI = \frac{z(SurINT) + z(DT)}{std(z(SurINT) + z(DT))} \tag{1}$$

where *std* is the standard deviation and *z* is the standardization of surplus intensity (SurINT) and deficit time (DT). Surplus intensity is the annual mean of daily surplus (in mm) intensity events for days when precipitation > ETo. In simple terms, surplus intensity can be defined as "excess water," with more water leading to potential extreme hydrologic events such as floods. In agroecosystems, periods of excessive rainfall can reduce crop productivity, sometimes by an amount comparable to severe drought (Dold et al., 2017; Yin et al., 2020). In many ecosystems, larger and more intense rain events can reduce net primary productivity (Post & Knapp, 2020) and/or decrease the ratio of rainfall to net primary production, especially when heavy rainfall events are separated by longer dry spells (Felton et al., 2021; Zhang et al., 2013). Deficit time is the annual mean dry spell length (in days) for days when precipitation < ETo. Deficit time represents the time of declining water availability, either for water resources or vegetation. For ecosystems, longer periods of water limitation are particularly concerning due to the potential for interactions between declining soil moisture and rising atmospheric VPD which can stress plants from the perspective of both water supply and atmospheric demand (Humphrey et al., 2021). Longer periods of water limitation also have increased the prevalence and duration of no flow conditions in streams, causing some perennial systems to shift to intermittent flow (Zipper et al., 2021).

To estimate SDI, annual surplus intensity and deficit time are standardized (*z*-score) using the 1950–1980 time period to allow for spatial and temporal comparability. The denominator in Equation 1, which is fixed temporally, allows SDI to be compared between regions with different climates (and thus different supply and demand characteristics). For historical evaluation and the projected changes for surplus intensity and deficit time, we present the results in their absolute values (mm or days) or percent change from the baseline time period to aid in interpretability.
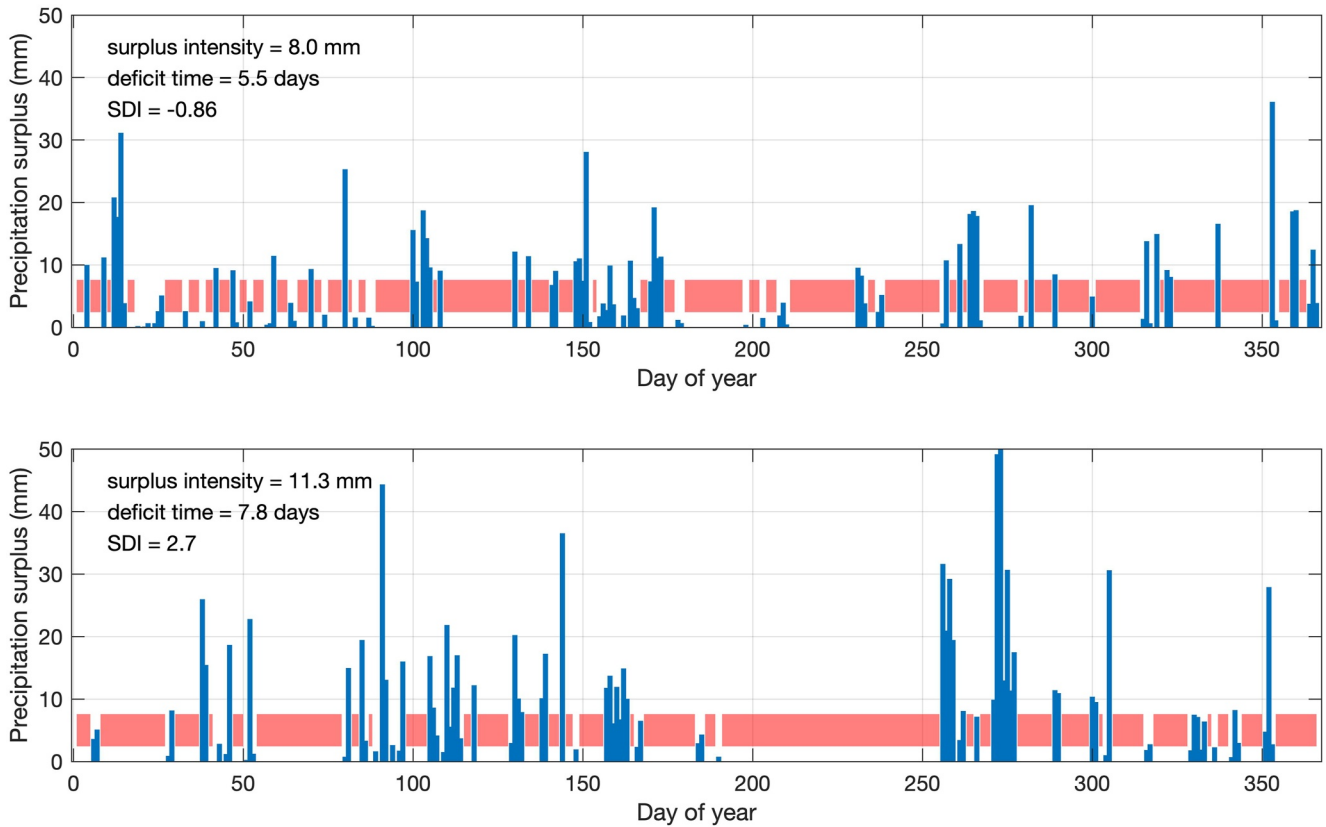
Figure 1. An example of the hydrological intensity index used in this study for the 36°N, 90°W grid point for the NorESM-LM climate model historical run. The top panel represents a non-hydrologically intense year during the historical time period, while the bottom panel represents a hydrologically intense year during the 2070–2100 time period. The transparent, red blocks indicate consecutive deficit days where precipitation is greater than reference evapotranspiration.

The *z*-scores of surplus intensity and deficit time are combined to express hydrological intensification or SDI (Equation 1). A large, positive SDI represents intensification via extreme precipitation surplus events, extended periods of water deficit, or a combination of both, while a negative SDI value represents low-intensity surplus precipitation events, small periods of water deficit, or a combination of both. While we largely focus on assessing changes of SDI and its underlying components as well as their relationship to water resource management, increased co-occurring precipitation surplus events and dry spells have been found, among others, to increase landslide events (Tichavský et al., 2019), result in crop damage (Barron et al., 2003), decrease dryland productivity (Felton et al., 2021), affect water quality (Loecke et al., 2017), increase wildfire activity (Flannigan & Harrington, 1988), and lead to unexpected impacts in coupled human and natural systems (J. Liu et al., 2007). An example of SDI is shown in Figure 1, where the bottom panel represents a more hydrologically intense year than the top panel (negative SDI value). Detailed background information on surplus intensity, deficit time, and SDI can be found in Ficklin et al. (2019).

Like most widely used metrics to describe drought status or to predict patterns of hydrological intensification, SDI is a simplification of a complex hydrological process, representing both wet and dry extremes. For example, SDI does not consider initial soil moisture content or water storage conditions, and therefore assumes that precipitation surplus events are completely converted into surface water runoff. In reality, precipitation surplus events may not be converted to water runoff if the initial soil moisture conditions are dry. Surplus intensity, however, could be an indicator of an event that increases soil moisture that would perhaps eventually lead to surface runoff. Additionally, ETo and the actual evapotranspiration that depletes soil moisture may become decoupled as ETo increases (especially in water-limited environments; McVicar et al., 2012) due to changes in water supply (Kauwe et al., 2017; Ohta et al., 2008; Peng et al., 2019), evaporative demand (Novick et al., 2016), or phenological vegetation characteristics (Donohue et al., 2010; C. Liu et al., 2017), of which are not completely characterized using SDI.

Table 1
CMIP6 GCMs Used in This Study

ID	Model name	Institution	Ensemble member	References
1	ACCESS-CM2	Commonwealth Scientific and Industrial Research Organization/Queensland Climate Change Center of Excellence, Australia	r1i1p1f1	Bi et al. (2020)
2	ACCESS-ESM1-5	Commonwealth Scientific and Industrial Research Organization/Queensland Climate Change Center of Excellence, Australia	r1i1p1f1	Ziehn et al. (2020)
3	BCC-CSM2-MR	Beijing Climate Center, China Meteorological Administration	r1i1p1f1	Wu et al. (2019)
4	CanESM5	Canadian Center for Climate Modeling and Analysis	r1i1p1f1	Swart et al. (2019)
5	CMCC-CM2-SR5	Euro-Mediterranean Center on Climate Change, Italy	r1i1p1f1	Cherchi et al. (2019)
6	CNRM-CM6-1	National Center of Meteorological Research, France	r1i1p1f2	Voldoire et al. (2019)
7	GFDL-ESM4	NOAA Geophysical Fluid Dynamics Laboratory, USA	r1i1p1f1	Dunne et al. (2020)
8	INM-CM5-0	Institute for Numerical Mathematics, Russia	r1i1p1f1	Volodin and Gritsun (2018)
9	MPI-ESM1-2-HR	Max Planck Institute, Germany	r1i1p1f1	Müller et al. (2018)
10	MPI-ESM1-2-LR	Max Planck Institute, Germany	r1i1p1f1	Mauritsen et al. (2019)
11	MRI-ESM2-0	Meteorological Research Institute, Japan	r1i1p1f1	Yukimoto et al. (2019)
12	NorESM2-LM	Norwegian Climate Center, Norway	r1i1p1f1	Seland et al. (2020)
13	NorESM2-MM	Norwegian Climate Center, Norway	r1i1p1f1	Seland et al. (2020)

2.2. Climate Model Ensemble

To estimate projected changes in terrestrial hydrological intensity, daily CMIP6 output from 13 global climate models (GCMs) was extracted from the CMIP6 data clearinghouse at https://esgf-node.llnl.gov/search/cmip6/. The CMIP6 ensemble has increased representations of physical processes and their horizontal and vertical resolution (Eyring et al., 2016). Models from CMIP6 span a wider range of warming and precipitation responses compared to CMIP5 models (Almazroui et al., 2020; Cook et al., 2020; Smith & Forster, 2021; Tebaldi et al., 2021; Tokarska et al., 2020).

We specifically extracted data for the *historical* (1850–2014) time period simulations that include climate forcings from natural and anthropogenic sources (Eyring et al., 2016). For the projected time period (2015–2100), we used GCM output (one ensemble member from each GCM) from two SSPs (O'Neill et al., 2016; SSP2-4.5 and SSP5-8.5). The SSPs differ based on socioeconomic assumptions and each SSP represents different radiative pathways resulting in a different radiative increase at the end of 2100, where SSP2-4.5 = 4.5 W/m^2 (moderate emissions) and SSP5-8.5 = 8.5 W/m^2 (high emissions). These represent approximate end-of-the 21st century average annual temperature increases of approximately 3°C and 5°C, respectively, compared to pre-industrial conditions (Cook et al., 2020; Tebaldi et al., 2021). We focus primarily on the results from the SSP2-4.5 forcing, but provide context for changes obtained with the SSP5-8.5 forcing.

For the historical and projected time periods, we used ensembles of opportunity based on specific models and ensemble members (found in Table 1) that provided the climate variables needed to calculate surplus intensity, deficit time, and SDI. Not all variables were available for the full 1850–2100 time period (some started in 1950), and thus the baseline for this work is defined as 1950–1980. All GCM output was bi-linearly interpolated to a common 1.5° grid. To ensure the reliability of the GCM projections, we evaluate the accuracy of the GCM ensemble against reanalysis data sets for 1979–2014. We find the GCM ensemble can adequately represent historical precipitation, ETo, surplus intensity, and deficit time. A detailed analysis is shown in Tables S1 and S2 and Figure S1 in Supporting Information S1.

2.3. Projected Changes in Terrestrial Hydrological Intensification

We compare GCM ensemble mean changes for surplus intensity, deficit time, SDI, precipitation event intensity (amount of precipitation per event [defined as >1 mm]), and daily ETo for one future time period (2070–2100) and SSPs 2-4.5 and 5-8.5 compared to the baseline period. We also examine the robustness of the change in intensification amongst GCMs for each grid cell, where a robust finding has agreement on the sign of the change by

at least 75% of the models (Scheff et al., 2021). To understand the relative influence of changes in precipitation and ETo on hydrological intensification, each climate variable was linearly detrended from 1950 to 2100 under SSP5-8.5, and the hydrological intensification metrics were re-assessed using one detrended climate variable and one raw (or unmodified) climate variable. For this, SSP5-8.5 was used because it exhibits the most extreme changes in temperature and precipitation, and thus the detrended signal is likely to be more apparent.

2.4. River Basin Data

While it has long been understood that the hydrologic cycle is intensifying, leading to grave implications for water management (Milly et al., 2008), understanding the co-occurrence of water surplus and deficits within years and across river basins is needed to adapt water management to climate change. Surplus intensity, deficit time, and SDI provide simple metrics to integrate precipitation surplus events and dry spells within the same year. These metrics quantify changes to evaluate the magnitude of hydrological intensification and whether changes are dominated by water surpluses or deficits. We identify potential future water management challenges by summarizing results for major global river basins that have significant water resources infrastructure. While SDI is a simplification of complex hydrological processes, quantifying the relationship between hydrological intensification (and corresponding metrics) is a crucial first step toward improving understanding of hydrological intensification effects on future water resources management decisions.

River basin descriptive information was extracted from HydroATLAS (Linke et al., 2019), which is a global data set of basin demographic and environmental characteristics. We focused on two variables in the HydroAT-LAS database that are directly related to water management: population (Center for International Earth Science Information Network - CIESIN - Columbia University, 2018) and percent area irrigated (Siebert et al., 2015). Additionally, the number of total endangered and threatened fish species was examined (IUCN, 2021) and then integrated with the HydroATLAS database. For this work, we relate changes in SDI to potential water resource management conflicts, as the magnitudes of precipitation and ETo are dominate factors that determine how precipitation is partitioned into runoff or evapotranspiration (Berghuijs et al., 2017; Blöschl et al., 2013; Budkyo, 1974), especially when summarized at the annual time step.

3. Results and Discussion

3.1. Global Hydrological Intensification

Our results suggest that precipitation surpluses are projected to increase, even after accounting for increases in evaporative demand. It is important to reiterate, though, that this work uses a version of ETo that incorporates the influence of CO_2 and VPD on stomatal conductance (as fully described in Yang et al. [2019]). As expected, and was found in previous work (Greve et al., 2019; Yang et al., 2019), not incorporating the influence of CO_2 and VPD on stomatal conductance resulted in a larger increase in ETo (Figures S2 and S3 in Supporting Information S1). This increased globally averaged surplus intensity (1%–2% without ETo that incorporates the influence of CO_2 and VPD compared to ETo with CO_2 and VPD), deficit time (2%–5% increase), and SDI (~0.1 increase in *z*-score) with larger changes found in drier regions (as found in Cui et al. [2021]). Regardless of whether the influence of CO_2 and VPD on stomatal conductance is incorporated in ETo, the changes in surplus intensity, deficit time, and SDI do not change sign and follow the same statistical significance as changes with the influence of CO_2 and VPD as is discussed in more detail below.

For the 2070–2100 time period, we find an 11.5 ± 4.6% (GCM ensemble mean and interquartile range) and 18.5 ± 4.7% increase in surplus intensity under SSP2-4.5 and SSP5-8.5, respectively, relative to the 1950–1980 baseline, with a robust agreement amongst GCMs (75.6% of the terrestrial surface for SSP2-4.5 and 80.1% for SSP5-8.5; Figure 2 for SSP2-4.5 and Figure S4 in Supporting Information S1 for SSP5-8.5). For both SSPs, the largest increases in surplus intensity occur in the northern and midlatitudes and generally follow patterns of increased precipitation event intensity (Figures 3 and S5 in Supporting Information S1; significant [$p < 0.05$] GCM ensemble mean Spearman correlation of 0.60 for SSP2-4.5 and 0.61 for SSP5-8.5). At the global scale, the CMIP6 ensemble generally predicts increases in precipitation event intensity for both SSPs (7.5% for SSP2-4.5 and 12.1% for SSP5-8.5) relative to baseline conditions (Figures 3 and S5 in Supporting Information S1), consistent with previous work using CMIP6 models (Cook et al., 2020; Tebaldi et al., 2021). Only India has consistent decreases in ETo, a result consistent in other studies that show projected decreases in drought for this region
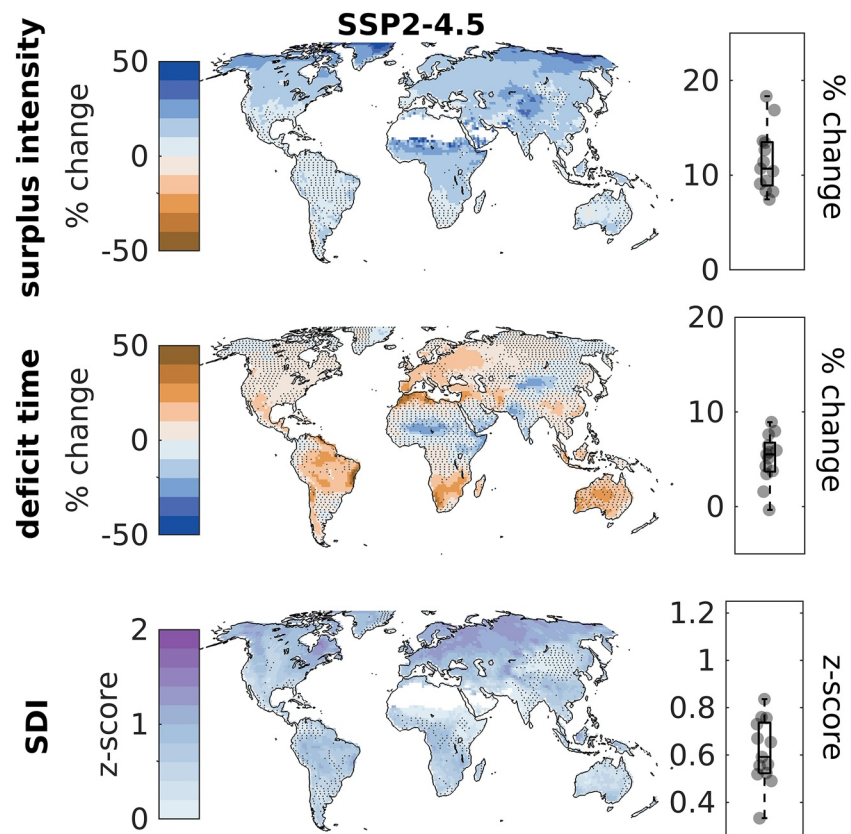
Figure 2. Projected changes in surplus intensity, deficit time, and surplus deficit intensification (SDI) for the 2070–2100 time period for the global climate model (GCM) ensemble mean under SSP2-4.5 relative to the 1950–1980 baseline. Map dots indicate a non-robust change (less than 75% of the models agree on the sign of the change). The scatter box plots represent the corresponding distribution of terrestrial average projections of surplus intensity, deficit time, and SDI for GCMs. Missing data (the white regions in the top and bottom panels) represent areas where surplus intensity (and thus SDI) cannot be estimated because surplus intensity events do not occur at some point during the baseline time period.

(Aadhar & Mishra, 2020; Cook et al., 2012). Both SSPs show more widespread increases in surplus intensity than average precipitation intensity, suggesting that precipitation events that eclipse ETo are projected to become more frequent and intense (Figures 2 and S4 in Supporting Information S1). Global average projections of precipitation event intensity, daily ETo, and hydrological intensification components can be found in Figure S6 in Supporting Information S1.

Even while surplus intensity is projected to increase globally under climate change, dry spell deficit time is also projected to lengthen (Figure 2 for SSP2-4.5 and Figure S4 in Supporting Information S1 for SSP5-8.5). Overall, for SSP2-4.5 and SSP5-8.5, GCM ensemble mean deficit time increased by approximately $5.1 \pm 3.1\%$ and $9.6 \pm 7.2\%$, with an area of robust change of 31.0% and 41.1%, respectively. Significant increases in deficit time occur in eastern North America, the Amazon region, southern Africa, and large portions of Europe and western Asia. These areas are where average daily ETo is projected to have a significant relative increase (>10%) and are coupled with minor changes or decreases in average precipitation event intensity (Figure 3). Changes in both average precipitation intensity and daily ETo are significantly ($p < 0.05$) correlated to changes in deficit time. Spearman correlation between late 21st century changes in precipitation event intensity and deficit time was −0.48 for SSP2-4.5 and −0.58 for SSP5-8.5, whereas the correlation between changes in daily ETo and deficit time was 0.25 for SSP2-4.5 and 0.34 for SSP5-8.5 (both significant at $p < 0.05$).

SDI generally follows the same spatial patterns and magnitudes as surplus intensity and deficit time with increases for much of the terrestrial surface (Figure 2 for SSP2-4.5 and Figure S4 in Supporting Information S1 for SSP5-8.5). For SSP2-4.5 and SSP5-8.5, we find an increase in SDI for the global terrestrial surface with a 0.61 ± 0.21 and 0.88 ± 0.24 z-score increase, respectively, with large areas of robust agreement for both SSPs. We
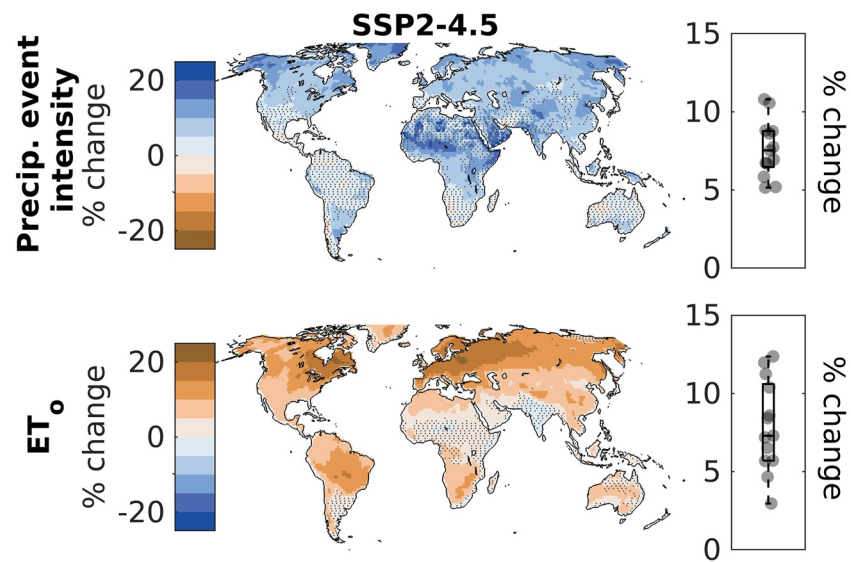
Figure 3. Projected changes in average precipitation event intensity and daily reference evapotranspiration (ETo) for the 2070–2100 time period for the global climate model (GCM) ensemble mean under SSP2-4.5 relative to the 1950–1980 baseline. Map dots indicate a nonrobust change (less than 75% of the models agree on the sign of the change). The scatter box plots represent the corresponding distribution of terrestrial average projections of precipitation and ETo for GCMs.

find a significant negative correlation (−0.56 for SSP2-4.5 and −0.61 for SSP5-8.5) between changes in surplus intensity and changes in deficit time, suggesting that hydrological intensification tends to be dominated by shifts in either precipitation surpluses or deficit time. Nonetheless, approximately two-thirds of the terrestrial surface shows an increase in both surplus intensity and deficit time for SSP2-4.5 and SSP5-8.5. The northern latitudes are projected to have the largest hydrological intensification (z-score increase >1), where large increases in surplus and moderate increases in deficit time are found. Only small portions of sub-Saharan Africa, India, and central Asia show reduced SDI by the end of this century, perhaps driven by changes in wet and dry season characteristics from increased atmospheric warming (Dong & Sutton, 2015; Dunning et al., 2018).

We re-assessed changes in hydrological intensification under SSP5-8.5 to understand the relative importance of individual trends in both precipitation and ETo in causing hydrological intensification. We find that detrending precipitation and keeping ETo at the original values results in slightly larger increases in hydrological intensification (global mean SDI z-score of 1.04) with the biggest differences were found in the midlatitudes and northern latitudes, driven by increases in surplus intensity after detrending as well as increases in deficit time in portions of Asia (Figure S7 in Supporting Information S1). Detrending ETo and keeping precipitation at its original values results in a decrease in hydrological intensification (terrestrial global SDI z-score of 0.62). As was the case for detrended precipitation, the largest differences were found in the midlatitudes and northern latitudes; however, the reason largely stemmed from a lack of increase in surplus intensity with deficit time overall playing a smaller role (Figure S7 in Supporting Information S1).

While detrending precipitation did result in an increase in hydrological intensification, many of the increases were smaller when compared to the large decreases for SDI with a detrended ETo. For many grid points, detrending ETo changed the direction of hydrological intensification from an increase to a decrease, as is shown in Figure 4. An increase in hydrological intensification from a detrended precipitation is counterintuitive; however, this result indicates that when precipitation is detrended many of the smaller precipitation events no longer eclipse ETo, and because we find an increase in precipitation event intensity for much of the terrestrial surface (Figures 4 and S5 in Supporting Information S1), this results in a lower number of small precipitation events that are included in the annual average of surplus intensity (4.8% reduction), thus resulting in an increase in surplus intensity magnitude. Additionally, with precipitation detrended, deficit time increased because the smaller precipitation events that broke up dry spells were no longer included (Figure 4). Similarly, when ETo is detrended (which increased for much of terrestrial surface; Figures 4 and S5 in Supporting Information S1), smaller precipitation events that eclipse ETo are included (10.4% increase), resulting in a decrease in the surplus intensity annual average. These
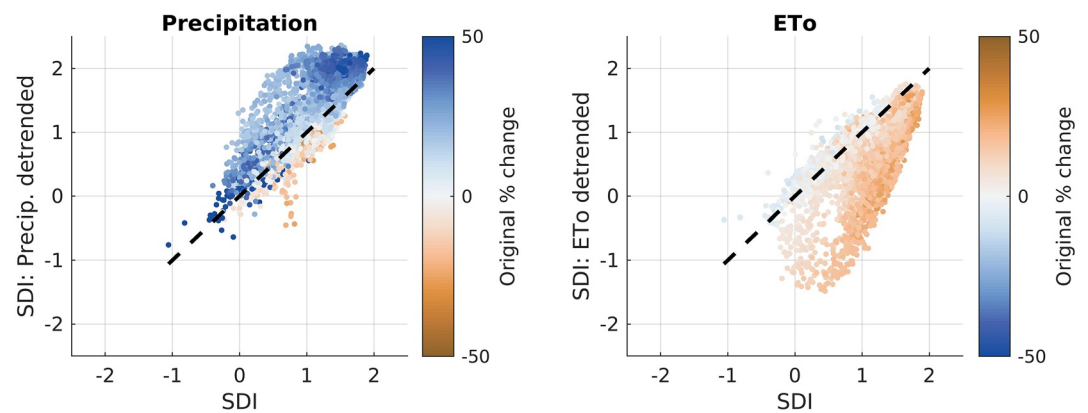
Figure 4. Scatterplot of surplus deficit intensification (SDI) of terrestrial grid points from the original global climate model (GCM) ensemble mean against SDI from the GCM ensemble mean with detrended precipitation (left) and ETo (right) under SSP5-8.5. The colors for each panel represent the percent change for the 2070–2100 time period for the original GCM ensemble mean under SSP5-8.5 relative to the 1950–1980 baseline. The black dashed line represents the 1:1 line and values near this line indicate that detrending did not result in a change in SDI.

smaller events tend to break up time periods where ETo > precipitation intensity, thus also decreasing in average deficit time. Additionally, defining hydrological intensification using precipitation and atmosphere demand led to more intensification as compared to solely using precipitation (as is found in Giorgi et al. [2011]). For the global average, incorporating atmospheric demand increased projected surplus intensity by ∼3%–4%, deficit time by 3%–4%, and SDI by 0.25 (not shown).

3.2. Implications and Recommendations for Water Resource Management

An increase in surplus intensity events suggests the possibility of more flooding (Blöschl et al., 2019; Davenport et al., 2021; Mallakpour & Villarini, 2015) with subsequent impacts to soil moisture and groundwater recharge (Cook et al., 2020; Mankin et al., 2019; Smerdon, 2017), water quality (Wheater & Evans, 2009), biodiversity, and ecosystem health (Maestre et al., 2015). Additionally, Famiglietti et al. (2021) found that extreme wet events are just as important as extreme dry events for controlling vegetation green-up anomalies. These impacts, in turn, affect other hydrologic variables such as infiltration and evapotranspiration. Increases in deficit time are a common proxy for droughts (Vicente-Serrano et al., 2010), flash droughts (Mo & Lettenmaier, 2016; Otkin et al., 2018), increased wildfire potential (Flannigan & Harrington, 1988), decreased streamflow (Ficklin et al., 2018), and groundwater resilience (Hahm et al., 2019). Persistence and lengthening of dry conditions can force a transition from a system limited by energy to a system that is limited by water, leading to increased vegetation stress (McDowell et al., 2008), plant mortality (Allen et al., 2010), and potential species composition change (Bréda et al., 2006; Trugman et al., 2020). It is important to note, though, that we summarize hydrological intensification at the annual time scale and therefore do not distinguish hydrological intensification within seasons. Regardless, either increasing surplus intensity or lengthening deficit times can impact natural and built systems; the fact that they occur together within the same year for most of the land surface signifies a concerning departure from historical conditions.

An increase in SDI influences the timing, location, and amount of water available for cities, industry, agriculture, and ecosystems, where periods of too much water may be followed by extensive periods without water. Existing research has focused on long-term trends of climate change on water resources (Schewe et al., 2014) and future inter-annual variability for water allocation (Null & Viers, 2013). However, hydrological intensification is likely to challenge water management since water resources management often relies upon or assumes hydroclimate stationarity (Milly et al., 2008).

Generally, water infrastructure and water right/allocation frameworks have been designed to manage seasonal wet and dry periods. For example, dams are built to store wet season runoff for dry season water supply, irrigation, and sometimes environmental flows. In climate types defined by distinct wet and dry seasons like Mediterranean, tropical savannah, monsoon-influenced climates, and some midlatitude and semi-arid climates, variability in
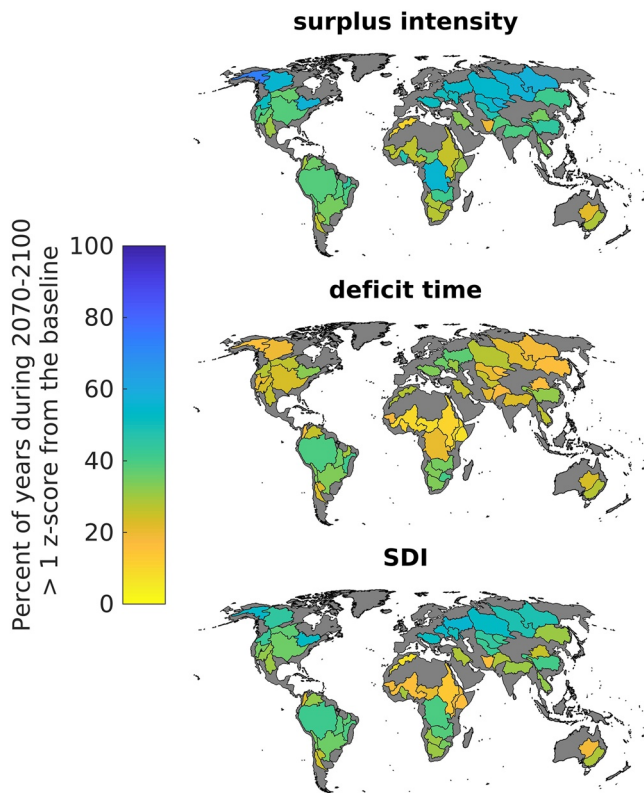
Figure 5. Major global river basins and the percent of years during the 2070–2100 time period under SSP2-4.5 that have an ensemble mean z-score >1 z-score compared to the historical baseline (1950–1980) for surplus intensity, deficit time, and surplus deficit intensification (SDI).

seasonal precipitation is more certain than variability among years. Similarly, climate types that historically did not have precipitation seasonality may increasingly experience precipitation surpluses and deficit periods at the end of the 21st century that are challenging to predict and manage (Figures 2 and S4 in Supporting Information S1).

To better quantify water management-relevant shifts, we summarize the GCM ensemble mean SDI results under SSP2-4.5 (moderate emissions scenario) for major river basins throughout the world that have considerable surface reservoir capacity (Lehner et al., 2011; Figure 5; Figures S8–S9 in Supporting Information S1 for SSP5-8.5). For each of these basins, we examine the percent of years in the 2070–2100 time period that have an SDI z-score >1, which gives an indication of the number of hydrologically intense years that may lead to complex or unprecedented water resource management. An example of an SDI year >1 is the Sacramento River Basin in northern California during 2012. In late 2012, in the midst of a prolonged and severe drought, the Sacramento River Basin was hit with a series of major storms that resulted in floods, even though annual precipitation remained well below normal (US Drought Monitor, 2021).

For basins with considerable reservoir storage, we find that, on average, 34.1% of years (10.5 years) during the 2070–2100 time period have an SDI z-score >1 (Figure 5; the SSP5-8.5 pathway results in 44.5% of years [13.8 years]) compared to only 11% (3.4 years) during the historical baseline. We also find that, on average, SDI z-scores >1 occur 1.7 years in consecutive duration (2.6 years for SSP5-8.5), further complicating water resource management. Of the 10.5 years between 2070 and 2100 with an SDI z-score >1, 3 of those years (4.9 years for SSP5-8.5) have both surplus and deficit time >1 z-score in a given year (baseline value = 0.6 years) and >0.5 z-score for 6 years (8.3 years for SSP5-8.5; baseline value = 2 years). These changes are largely driven by increases in surplus intensity >1 z-score, though basins such as the Amazon River Basin, show large percentages of time during 2070–2100 with a deficit time >1 z-score (Figure 5).

Basins with the most reservoir capacity are projected to have more hydrologically intense years (significant [p < 0.05] Spearman's correlation of 0.33; Figure 6). These basins with substantial reservoir capacity may be required to spill water from reservoirs during intense wet periods, followed by extended periods when they have numerous empty reservoirs but not enough precipitation to fill them (Hanak et al., 2011; van Dijk et al., 2013). Managing intense and perhaps unprecedented flood events will also challenge existing infrastructure and management (Independent Forensic Team Report–Oroville Dam Spillway Incident, 2018). Overall, managing infrastructure in these large basins to reduce flood risk and store water for extended drought will likely be contentious.

The heavily managed river basins with >40% of hydrologically intense years during the 2070–2100 time period include the Amazon River Basin, Danube River Basin, St. Lawrence River Basin, and the Yukon River Basin.
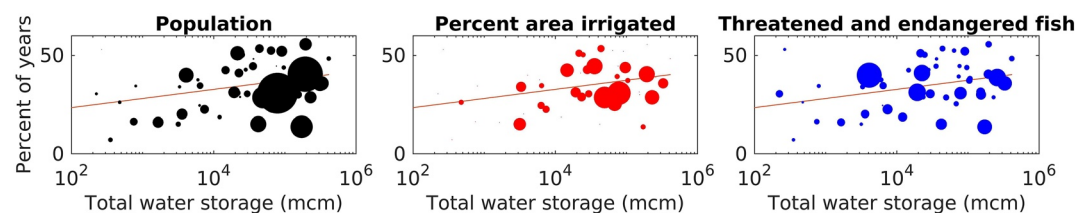

Figure 6. Scatterplots representing the relationship between total water storage (in million cubic meters; mcm) and the percent of years during 2071–2100 under SSP2-4.5 with surplus deficit intensification >1 z-score from the baseline. The size of the markers in each scatter plot shows the total population, percent area irrigated, and total number of threatened and endangered species within each basin.

Basins such as the Murray-Darling River Basin, Niger River Basin, and Nile River Basin have hydrologically intense years <20% of the time during the 2070–2100 time period, but still more than the historical time period (Figure 5). The reasons for these changes in hydrologically intense years vary from basin-to-basin. For example, hydrological intensification in the Amazon River Basin is largely a result of increased deficit time, while hydrological intensification in the Yukon River Basin is driven by large increases in surplus intensity (Figure 5). Previous research has shown that observed seasonal surface water storage variability is concentrated in arid and semiarid regions and south of 45° north latitude (Cooley et al., 2021). Here, we nuance this finding by showing that many heavily managed river basins in northern Europe, Asia, and North America will experience considerable hydrological intensification by the end of this century (Figure 5). Some basins that are hotspots for hydropower development, like the Amazon and Mekong River Basins (Barbarossa et al., 2020), are likely to have reduced generation as a result of hydrological intensification, particularly when intensification is driven by increased deficit time. River basins with considerable reservoir capacity are also basins with large populations (significant [$p < 0.05$] Spearman correlation with reservoir volume = 0.42), land irrigated with ground or surface water (correlation = 0.19), and threatened and endangered aquatic species (significant correlation = 0.32), suggesting that water in these basins must be allocated amongst these three sectors (Figure 6). Similarly, the basins with >40% of hydrologically intense future years currently have, on average, greater populations, irrigated land, and threatened and endangered species, compared to basins with <20% of hydrologically intense years. This implies that hydrological intensification among urban, agricultural, and environmental water uses will likely lead to conflict among water sectors.

Depending on water rights structures, water shortages may be shared among users, or water may be allocated based on water right priority. Agricultural water users generally receive the most water, while urban water users value water the highest. Water markets sometimes transfer water from agricultural to urban or environmental water uses (Grafton et al., 2013). Urban water suppliers value water reliability and often stress test systems so they have a good understanding of future risk and promising options to obtain extra water before droughts (Brown et al., 2012). Managed environmental water allocations are typically small and are further reduced during droughts, so environmental flows may be inadequate to preserve species and ecosystems during prolonged or persistent droughts (Grafton et al., 2013; Null & Viers, 2013). Ecosystem management tends to be reactive to hydrological intensification, with little planning before floods and droughts (Lund et al., 2018).

Our findings beg the question, to what extent is water management infrastructure ready for a more hydrologically intense future? Hydrological intensification could be alleviated to some extent in basins with large reservoirs that provide multiyear storage, although reservoirs sometimes lead to counter-intuitive outcomes like increasing water demand and vulnerability (Di Baldassarre et al., 2018). The dependence on mountain water storage in the form of snow may further complicate water resource management (Livneh & Badger, 2020), as the shift from snow-to-rain may decrease snowpack water storage in mountainous regions where hydrological intensification is the highest. Promising solutions to recurrent drought from increasing deficit time are likely varied but may include combinations of conjunctive use of surface and groundwater (Scanlon et al., 2016), prioritizing water conveyance to improve flexibility in basins with substantial surface storage (Null, 2016), stormwater and floodplain management (Palmer et al., 2008), and perhaps new surface or underground storage (Ehsani et al., 2017). Incorporating weather forecasts into reservoir operations may improve water management with precipitation surplus events (Alexander et al., 2021). In general, building flexibility into water infrastructure and management is an adaptation for hydrological intensification (Gersonius et al., 2013) and could include modifying dam operations (Ehsani et al., 2017), revising flood operating rules (Willis et al., 2011), or incorporating climate projections into flood risk mitigation (Sims & Null, 2019).

In highly managed river basins, hydrological intensification could result in flood and drought events that are beyond infrastructure design specifications (Raymond et al., 2020). Historic floods and droughts will be invaluable to understand and mitigate risk, although we show that future events may be more intense, more frequent, or longer. Understanding the drivers behind hydrological intensification, quantified here as increasing deficit time or an increase in surplus intensity, will also be useful to plan and assess risk. Hydrological intensification alternatives should be incorporated into regional or watershed-scale water resources management research to evaluate specific climate adaptation strategies and understand the limitations of existing infrastructure to manage more intense flood or drought periods. Our study identifies major river basins that are priorities for this future work. Overall, our findings suggest that the common practice of modeling effects of climate-induced *annual*

temperature and precipitation changes for water management may underprepared us for more severe climate intensification events that will stress water infrastructure and management.

4. Conclusions

Our results indicate that the hydrological cycle will continue to intensify into the future. Globally, these changes are driven largely by increases in precipitation surplus events (+11.5% for a moderate emissions scenario by the end of the century; +18.5% for a high emissions scenario), with increases in deficit time overall playing a smaller role (+5.1%; +9.6%). This leads to major river basins in northern latitudes, sub-Saharan Africa, and other regions that are projected to experience large increases in intensification due to precipitation surplus events. However, some important water resource regions (such as the Amazon River Basin) show that increases in deficit time will dominate hydrological intensification in the future. In sum, these changes are expected to increase the number of hydrologic extremes within a given year, resulting in increased stress on existing water resource infrastructure. Consequently, we find that the river basins with the largest water storage are also projected to have the strongest hydrological intensification with some basins (generally found in the northern latitudes) having three times more hydrologically intense years than the historical baseline. This indicates that in the future, water resource managers in areas with extreme hydrological intensification must balance between storing and/or releasing water for agricultural, ecological, and urban sectors in the face of increasing hydrologic extremes and must therefore incorporate flexibility into water resource infrastructure and management.

Data Availability Statement

The CMIP6 model outputs are available from the CMIP6 archive at: https://pcmdi.llnl.gov/CMIP6/. Specifically, the authors acknowledge Bi et al. (2020), Cherchi et al. (2019), Dunne et al. (2020), Mauritsen et al. (2019), Müller et al. (2018), Seland et al. (2020), Swart et al. (2019), Voldoire et al. (2019), Volodin and Gritsun (2018), Wu et al. (2019), Yukimoto et al. (2019), and Ziehn et al. (2020). Multisource Weighted-Ensemble Precipitation Version 2 (Beck et al., 2017) can be acquired via http://www.gloh2o.org/mswep/. NCEP-NCAR reanalysis data (Kalnay et al., 1996) can be acquired via https://psl.noaa.gov/data/gridded/data.ncep.reanalysis.html. MERRA-2 data (Gelaro et al., 2017) can be acquired via https://gmao.gsfc.nasa.gov/reanalysis/MERRA-2/. ERA-Interim reanalysis data (Dee et al., 2011) can be acquired via https://www.ecmwf.int/en/forecasts/datasets/reanalysis-datasets/era-interim. HydroATLAS (Linke et al., 2019) can be acquired via https://www.hydrosheds.org/page/hydroatlas. International Union for the Conservation of Nature threatened and endangered species can be acquired via https://www.iucnredlist.org/resources/spatial-data-download. Code to estimate the hydrological intensification metrics from Ficklin et al. (2019) can be found on Zenodo at: https://zenodo.org/record/5092873#.YOxfBG4pBGM; https://doi.org/10.5281/zenodo.5092873.

References

Aadhar, S., & Mishra, V. (2020). On the projected decline in droughts over South Asia in CMIP6 multimodel ensemble. *Journal of Geophysical Research: Atmospheres*, *125*(20), e2020JD033587. https://doi.org/10.1029/2020JD033587

Ainsworth, E. A., & Rogers, A. (2007). The response of photosynthesis and stomatal conductance to rising CO2: Mechanisms and environmental interactions. *Plant, Cell and Environment*, *30*(3), 258–270. https://doi.org/10.1111/j.1365-3040.2007.01641.x

Alexander, S., Yang, G., Addisu, G., & Block, P. (2021). Forecast-informed reservoir operations to guide hydropower and agriculture allocations in the Blue Nile basin, Ethiopia. *International Journal of Water Resources Development*, *37*(2), 208–233. https://doi.org/10.1080/07900627.2020.1745159

Allan, R. P., Barlow, M., Byrne, M. P., Cherchi, A., Douville, H., Fowler, H. J., et al. (2020). Advances in understanding large-scale responses of the water cycle to climate change. *Annals of the New York Academy of Sciences*, *1472*(1), 49–75. https://doi.org/10.1111/nyas.14337

Allen, C. D., Macalady, A. K., Chenchouni, H., Bachelet, D., McDowell, N., Vennetier, M., et al. (2010). A global overview of drought and heat-induced tree mortality reveals emerging climate change risks for forests. *Forest Ecology and Management*, *259*(4), 660–684. Retrieved from https://www.sciencedirect.com/science/article/pii/S037811270900615X

Allen, M. R., & Ingram, W. J. (2002). Constraints on future changes in climate and the hydrologic cycle. *Nature*, *419*(6903), 224–232. https://doi.org/10.1038/nature01092

Almazroui, M., Saeed, F., Saeed, S., Islam, M. N., Ismail, M., Klutse, N. A. B., & Siddiqui, M. H. (2020). Projected change in temperature and precipitation over Africa from CMIP6. *Earth Systems and Environment*, *4*(3), 455–475. https://doi.org/10.1007/s41748-020-00161-x

Barbarossa, V., Schmitt, R. J., Huijbregts, M. A., Zarfl, C., King, H., & Schipper, A. M. (2020). Impacts of current and future large dams on the geographic range connectivity of freshwater fish worldwide. *Proceedings of the National Academy of Sciences of the United States of America*, *117*(7), 3648–3655. https://doi.org/10.1073/pnas.1912776117

Barron, J., Rockström, J., Gichuki, F., & Hatibu, N. (2003). Dry spell analysis and maize yields for two semi-arid locations in east Africa. *Agricultural and Forest Meteorology*, *117*(1–2), 23–37. https://doi.org/10.1016/s0168-1923(03)00037-6

Beck, H. E., van Dijk, A. I. J. M., Levizzani, V., Schellekens, J., Miralles, D. G., Martens, B., & de Roo, A. (2017). MSWEP: 3-hourly 0.25° global gridded precipitation (1979–2015) by merging gauge, satellite, and reanalysis data. *Hydrology and Earth System Sciences*, *21*(1), 589–615. Retrieved from https://hess.copernicus.org/articles/21/589/2017/

Berghuijs, W. R., Larsen, J. R., Van Emmerik, T. H., & Woods, R. A. (2017). A global assessment of runoff sensitivity to changes in precipitation, potential evaporation, and other factors. *Water Resources Research*, *53*(10), 8475–8486. https://doi.org/10.1002/2017wr021593

Bi, D., Dix, M., Marsland, S., O'Farrell, S., Sullivan, A., Bodman, R., et al. (2020). Configuration and spin-up of ACCESS-CM2, the new generation Australian Community Climate and Earth System Simulator Coupled Model. *Journal of Southern Hemisphere Earth Systems Science*, *70*(1), 225–251. Retrieved from https://www.publish.csiro.au/paper/ES19040

Blöschl, G., Bloschl, G., Sivapalan, M., Wagener, T., Savenije, H., & Viglione, A. (Eds.). (2013). *Runoff prediction in ungauged basins: synthesis across processes, places and scales*. Cambridge University.

Blöschl, G., Hall, J., Viglione, A., Perdigão, R. A. P., Parajka, J., Merz, B., et al. (2019). Changing climate both increases and decreases European river floods. *Nature*, *573*(7772), 108–111. https://doi.org/10.1038/s41586-019-1495-6

Bréda, N., Huc, R., Granier, A., & Dreyer, E. (2006). Temperate forest trees and stands under severe drought: A review of ecophysiological responses, adaptation processes and long-term consequences. *Annals of Forest Science*, *63*(6), 625–644. https://doi.org/10.1051/forest:2006042

Brown, C., Ghile, Y., Laverty, M., & Li, K. (2012). Decision scaling: Linking bottom-up vulnerability analysis with climate projections in the water sector. *Water Resources Research*, *48*(9). https://doi.org/10.1029/2011WR011212

Budyko, M. I. (1974). *Climate and life*. Academic Press.

Center for International Earth Science Information Network - CIESIN - Columbia University. (2018). *Gridded population of the world, version 4 (GPWv4): Population count, Revision 11*. https://doi.org/10.7927/H4JW8BX5

Cherchi, A., Fogli, P. G., Lovato, T., Peano, D., Iovino, D., Gualdi, S., et al. (2019). Global mean climate and main patterns of variability in the CMCC-CM2 coupled model. *Journal of Advances in Modeling Earth Systems*, *11*(1), 185–209. https://doi.org/10.1029/2018MS001369

Cook, B. I., Bell, A. R., Anchukaitis, K. J., & Buckley, B. M. (2012). Snow cover and precipitation impacts on dry season streamflow in the Lower Mekong Basin. *Journal of Geophysical Research: Atmospheres*, *117*(D16), D16116. https://doi.org/10.1029/2012JD017708

Cook, B. I., Mankin, J. S., Marvel, K., Williams, A. P., Smerdon, J. E., & Anchukaitis, K. J. (2020). Twenty-first century drought projections in the CMIP6 forcing scenarios. *Earth's Future*, *8*(6), e2019EF001461. https://doi.org/10.1029/2019EF001461

Cooley, S. W., Ryan, J. C., & Smith, L. C. (2021). Human alteration of global surface water storage variability. *Nature*, *591*(7848), 78–81. https://doi.org/10.1038/s41586-021-03262-3

Cui, J., Yang, H., Huntingford, C., Kooperman, G. J., Lian, X., He, M., & Piao, S. (2021). Vegetation response to rising CO_2 amplifies contrasts in water resources between global wet and dry land areas. *Geophysical Research Letters*, *48*(14), e2021GL094293. https://doi.org/10.1029/2021gl094293

Davenport, F. V., Burke, M., & Diffenbaugh, N. S. (2021). Contribution of historical precipitation change to US flood damages. *Proceedings of the National Academy of Sciences of the United States of America*, *118*(4), e2017524118. Retrieved from https://www.pnas.org/content/pnas/118/4/e2017524118.full.pdf

Dee, D. P., Uppala, S. M., Simmons, A. J., Berrisford, P., Poli, P., Kobayashi, S., et al. (2011). The ERA-Interim reanalysis: Configuration and performance of the data assimilation system. *Quarterly Journal of the Royal Meteorological Society*, *137*(656), 553–597. Retrieved from https://rmets.onlinelibrary.wiley.com/doi/abs/10.1002/qj.828

Di Baldassarre, G., Wanders, N., AghaKouchak, A., Kuil, L., Rangecroft, S., Veldkamp, T. I. E., et al. (2018). Water shortages worsened by reservoir effects. *Nature Sustainability*, *1*(11), 617–622. https://doi.org/10.1038/s41893-018-0159-0

Dold, C., Büyükcangaz, H., Rondinelli, W., Prueger, J. H., Sauer, T. J., & Hatfield, J. L. (2017). Long-term carbon uptake of agro-ecosystems in the Midwest. *Agricultural and Forest Meteorology*, *232*, 128–140. https://doi.org/10.1016/j.agrformet.2016.07.012

Donat, M. G., Alexander, L. V., Yang, H., Durre, I., Vose, R., Dunn, R. J. H., et al. (2013). Updated analyses of temperature and precipitation extreme indices since the beginning of the twentieth century: The HadEX2 dataset. *Journal of Geophysical Research: Atmospheres*, *118*(5), 2098–2118. https://doi.org/10.1002/jgrd.50150

Dong, B., & Sutton, R. (2015). Dominant role of greenhouse-gas forcing in the recovery of Sahel rainfall. *Nature Climate Change*, *5*(8), 757–760. https://doi.org/10.1038/nclimate2664

Donohue, R. J., Roderick, M. L., & McVicar, T. R. (2010). Can dynamic vegetation information improve the accuracy of Budyko's hydrological model? *Journal of Hydrology*, *390*(1–2), 23–34. https://doi.org/10.1016/j.jhydrol.2010.06.025

Dunne, J. P., Horowitz, L. W., Adcroft, A. J., Ginoux, P., Held, I. M., John, J. G., et al. (2020). The GFDL Earth System Model Version 4.1 (GFDL-ESM 4.1): Overall coupled model description and simulation characteristics. *Journal of Advances in Modeling Earth Systems*, *12*(11). e2019MS002015. https://doi.org/10.1029/2019MS002015

Dunning, C. M., Black, E., & Allan, R. P. (2018). Later wet seasons with more intense rainfall over Africa under future climate change. *Journal of Climate*, *31*(23), 9719–9738. https://doi.org/10.1175/jcli-d-18-0102.1

Ehsani, N., Vörösmarty, C. J., Fekete, B. M., & Stakhiv, E. Z. (2017). Reservoir operations under climate change: Storage capacity options to mitigate risk. *Journal of Hydrology*, *555*, 435–446. Retrieved from https://www.sciencedirect.com/science/article/pii/S0022169417305991

Eyring, V., Bony, S., Meehl, G. A., Senior, C. A., Stevens, B., Stouffer, R. J., & Taylor, K. E. (2016). Overview of the Coupled Model Intercomparison Project Phase 6 (CMIP6) experimental design and organization. *Geoscientific Model Development*, *9*(5), 1937–1958. Retrieved from https://gmd.copernicus.org/articles/9/1937/2016/

Famiglietti, C. A., Michalak, A. M., & Konings, A. G. (2021). Extreme wet events as important as extreme dry events in controlling spatial patterns of vegetation greenness anomalies. *Environmental Research Letters*, *16*, 074014. https://doi.org/10.1088/1748-9326/abfc78

Felton, A. J., Shriver, R. K., Bradford, J. B., Suding, K. N., Allred, B. W., & Adler, P. B. (2021). Biotic vs abiotic controls on temporal sensitivity of primary production to precipitation across North American drylands. *New Phytologist*, *231*(6), 2150–2161. https://doi.org/10.1111/nph.17543

Felton, A. J., Slette, I. J., Smith, M. D., & Knapp, A. K. (2020). Precipitation amount and event size interact to reduce ecosystem functioning during dry years in a mesic grassland. *Global Change Biology*, *26*(2), 658–668. https://doi.org/10.1111/gcb.14789

Ficklin, D. L., Abatzoglou, J. T., & Novick, K. A. (2019). A new perspective on terrestrial hydrologic intensity that incorporates atmospheric water demand. *Geophysical Research Letters*, *46*(14), 8114–8124. https://doi.org/10.1029/2019GL084015

Ficklin, D. L., Abatzoglou, J. T., Robeson, S. M., Null, S. E., & Knouft, J. H. (2018). Natural and managed watersheds show similar responses to recent climate change. *Proceedings of the National Academy of Sciences of the United States of America*, *115*(34), 8553–8557. Retrieved from https://www.pnas.org/content/pnas/115/34/8553.full.pdf

Ficklin, D. L., & Novick, K. A. (2017). Historic and projected changes in vapor pressure deficit suggest a continental-scale drying of the United States atmosphere. *Journal of Geophysical Research: Atmospheres*. , *122*(4), 2061–2079. https://doi.org/10.1002/2016JD025855

Flannigan, M. D., & Harrington, J. B. (1988). A study of the relation of meteorological variables to monthly provincial area burned by wildfire in Canada (1953–80). *Journal of Applied Meteorology and Climatology*, *27*(4), 441–452. Retrieved from https://journals.ametsoc.org/view/journals/apme/27/4/1520-0450_1988_027_0441_asotro_2_0_co_2.xml

Flo, V., Martínez-Vilalta, J., Granda, V., Mencuccini, M., & Poyatos, R. (2021). Vapour pressure deficit is the main driver of tree canopy conductance across biomes. Preprint. https://doi.org/10.1002/essoar.10508049.1

Gelaro, R., McCarty, W., Suárez, M. J., Todling, R., Molod, A., Takacs, L., et al. (2017). The Modern-Era Retrospective Analysis for Research and Applications, Version 2 (MERRA-2). *Journal of Climate*, *30*(14), 5419–5454. Retrieved from https://journals.ametsoc.org/view/journals/clim/30/14/jcli-d-16-0758.1.xml

Gersonius, B., Ashley, R., Pathirana, A., & Zevenbergen, C. (2013). Climate change uncertainty: Building flexibility into water and flood risk infrastructure. *Climatic Change*, *116*(2), 411–423. https://doi.org/10.1007/s10584-012-0494-5

Giorgi, F., Im, E. S., Coppola, E., Diffenbaugh, N. S., Gao, X. J., Mariotti, L., & Shi, Y. (2011). Higher hydroclimatic intensity with global warming. *Journal of Climate*, *24*(20), 5309–5324. https://doi.org/10.1175/2011jcli3979.1

Grafton, R. Q., Pittock, J., Davis, R., Williams, J., Fu, G., Warburton, M., et al. (2013). Global insights into water resources, climate change and governance. *Nature Climate Change*, *3*(4), 315–321. https://doi.org/10.1038/nclimate1746

Greve, P., Orlowsky, B., Mueller, B., Sheffield, J., Reichstein, M., & Seneviratne, S. I. (2014). Global assessment of trends in wetting and drying over land. *Nature Geoscience*, *7*(10), 716–721. https://doi.org/10.1038/ngeo2247

Greve, P., Roderick, M. L., Ukkola, A. M., & Wada, Y. (2019). The aridity index under global warming. *Environmental Research Letters*, *14*(12), 124006. https://doi.org/10.1088/1748-9326/ab5046

Greve, P., & Seneviratne, S. I. (2015). Assessment of future changes in water availability and aridity. *Geophysical Research Letters*, *42*(13), 5493–5499. https://doi.org/10.1002/2015GL064127

Grossiord, C., Buckley, T. N., Cernusak, L. A., Novick, K. A., Poulter, B., Siegwolf, R. T., et al. (2020). Plant responses to rising vapor pressure deficit. *New Phytologist*, *226*(6), 1550–1566. https://doi.org/10.1111/nph.16485

Hahm, W. J., Dralle, D. N., Rempe, D. M., Bryk, A. B., Thompson, S. E., Dawson, T. E., & Dietrich, W. E. (2019). Low subsurface water storage capacity relative to annual rainfall decouples Mediterranean plant productivity and water use from rainfall variability. *Geophysical Research Letters*, *46*(12), 6544–6553. https://doi.org/10.1029/2019GL083294

Hanak, E., Lund, J., Dinar, A., Gray, B., Howitt, R., & Mount, J. (2011). *Managing California's water: From conflict to reconciliation*. Public Policy Institute of California.

He, X., & Sheffield, J. (2020). Lagged compound occurrence of droughts and pluvials globally over the past seven decades. *Geophysical Research Letters*, *47*(14), e2020GL087924. https://doi.org/10.1029/2020GL087924

Humphrey, V., Berg, A., Ciais, P., Gentine, P., Jung, M., Reichstein, M., et al. (2021). Soil moisture–atmosphere feedback dominates land carbon uptake variability. *Nature*, *592*(7852), 65–69. https://doi.org/10.1038/s41586-021-03325-5

Huntington, T. G., Weiskel, P. K., Wolock, D. M., & McCabe, G. J. (2018). A new indicator framework for quantifying the intensity of the terrestrial water cycle. *Journal of Hydrology*, *559*, 361–372. Retrieved from https://www.sciencedirect.com/science/article/pii/S0022169418301276

Independent Forensic Team Report–Oroville Dam Spillway Incident. (2018). Retrieved from https://www.ussdams.org/our-news/oroville-dam-spillway-incident-independent-forensic-team-final-report/

IUCN. (2021). *The IUCN red list of threatened species*. Version 2021-1. Retrieved from https://www.iucnredlist.org

Kalnay, E., Kanamitsu, M., Kistler, R., Collins, W., Deaven, D., & Gandin, L. (1996). The NCEP/NCAR 40-year reanalysis project. *Bulletin of the American Meteorological Society*, *77*(3), 437–472. https://doi.org/10.1175/1520-0477(1996)077<0437:tnyrp>2.0.co;2

Kauwe, M. G. D., Medlyn, B. E., Knauer, J., & Williams, C. A. (2017). Ideas and perspectives: How coupled is the vegetation to the boundary layer? *Biogeosciences*, *14*(19), 4435–4453. https://doi.org/10.5194/bg-14-4435-2017

Kirchmeier-Young, M. C., & Zhang, X. (2020). Human influence has intensified extreme precipitation in North America. *Proceedings of the National Academy of Sciences of the United States of America*, *117*(24), 13308–13313. Retrieved from https://www.pnas.org/content/pnas/117/24/13308.full.pdf

Lavers, D. A., Ralph, F. M., Waliser, D. E., Gershunov, A., & Dettinger, M. D. (2015). Climate change intensification of horizontal water vapor transport in CMIP5. *Geophysical Research Letters*, *42*(13), 5617–5625. https://doi.org/10.1002/2015GL064672

Lehner, B., Liermann, C. R., Revenga, C., Vörösmarty, C., Fekete, B., Crouzet, P., et al. (2011). High-resolution mapping of the world's reservoirs and dams for sustainable river-flow management. *Frontiers in Ecology and the Environment*, *9*(9), 494–502. https://doi.org/10.1890/100125

Linke, S., Lehner, B., Ouellet Dallaire, C., Ariwi, J., Grill, G., Anand, M., et al. (2019). Global hydro-environmental sub-basin and river reach characteristics at high spatial resolution. *Scientific Data*, *6*(1), 283. https://doi.org/10.1038/s41597-019-0300-6

Liu, C., Sun, G., McNulty, S. G., Noormets, A., & Fang, Y. (2017). Environmental controls on seasonal ecosystem evapotranspiration/potential evapotranspiration ratio as determined by the global eddy flux measurements. *Hydrology and Earth System Sciences*, *21*(1), 311–322. https://doi.org/10.5194/hess-21-311-2017

Liu, J., Dietz, T., Carpenter, S. R., Alberti, M., Folke, C., Moran, E., et al. (2007). Complexity of coupled human and natural systems. *Science*, *317*(5844), 1513–1516. https://doi.org/10.1126/science.1144004

Livneh, B., & Badger, A. M. (2020). Drought less predictable under declining future snowpack. *Nature Climate Change*, *10*(5), 452–458. https://doi.org/10.1038/s41558-020-0754-8

Loecke, T. D., Burgin, A. J., Riveros-Iregui, D. A., Ward, A. S., Thomas, S. A., Davis, C. A., & Clair, M. A. S. (2017). Weather whiplash in agricultural regions drives deterioration of water quality. *Biogeochemistry*, *133*(1), 7–15. https://doi.org/10.1007/s10533-017-0315-z

Lund, J., Medellin-Azuara, J., Durand, J., & Stone, K. (2018). Lessons from California's 2012-2016 drought. *Journal of Water Resources Planning and Management*, *144*(10), 04018067. https://doi.org/10.1061/(asce)wr.1943-5452.0000984

Maestre, F. T., Delgado-Baquerizo, M., Jeffries, T. C., Eldridge, D. J., Ochoa, V., Gozalo, B., et al. (2015). Increasing aridity reduces soil microbial diversity and abundance in global drylands. *Proceedings of the National Academy of Sciences of the United States of America*, *112*(51), 15684–15689. Retrieved from https://www.pnas.org/content/pnas/112/51/15684.full.pdf

Mallkpour, I., & Villarini, G. (2015). The changing nature of flooding across the central United States. *Nature Climate Change*, *5*(3), 250–254. https://doi.org/10.1038/nclimate2516

Mankin, J. S., Seager, R., Smerdon, J. E., Cook, B. I., & Williams, A. P. (2019). Mid-latitude freshwater availability reduced by projected vegetation responses to climate change. *Nature Geoscience*, *12*(12), 983–988. https://doi.org/10.1038/s41561-019-0480-x

Mauritsen, T., Bader, J., Becker, T., Behrens, J., Bittner, M., Brokopf, R., et al. (2019). Developments in the MPI-M Earth System Model version 1.2 (MPI-ESM1.2) and its response to increasing CO2. *Journal of Advances in Modeling Earth Systems*, *11*(4), 998–1038. https://doi.org/10.1029/2018MS001400

McDowell, N., Pockman, W. T., Allen, C. D., Breshears, D. D., Cobb, N., Kolb, T., et al. (2008). Mechanisms of plant survival and mortality during drought: Why do some plants survive while others succumb to drought? *New Phytologist*, *178*(4), 719–739. https://doi.org/10.1111/j.1469-8137.2008.02436.x

McEvoy, D. J., Pierce, D. W., Kalansky, J. F., Cayan, D. R., & Abatzoglou, J. T. (2020). Projected changes in reference evapotranspiration in California and Nevada: Implications for drought and wildland fire danger. *Earth's Future*, *8*(11), e2020EF001736. https://doi.org/10.1029/2020ef001736

McVicar, T. R., Roderick, M. L., Donohue, R. J., Li, L. T., Van Niel, T. G., Thomas, A., et al. (2012). Global review and synthesis of trends in observed terrestrial near-surface wind speeds: Implications for evaporation. *Journal of Hydrology*, *416*, 182–205. https://doi.org/10.1016/j.jhydrol.2011.10.024

Medlyn, B. E., Duursma, R. A., Eamus, D., Ellsworth, D. S., Prentice, I. C., Barton, C. V. M., et al. (2011). Reconciling the optimal and empirical approaches to modelling stomatal conductance. *Global Change Biology*, *17*(6), 2134–2144. https://doi.org/10.1111/j.1365-2486.2010.02375.x

Milly, P. C. D., Betancourt, J., Falkenmark, M., Hirsch, R. M., Kundzewicz, Z. W., Lettenmaier, D. P., & Stouffer, R. J. (2008). Stationarity is dead: Whither water management? *Science*, *319*(5863), 573–574. Retrieved from https://science.sciencemag.org/content/sci/319/5863/573.full.pdf

Milly, P. C. D., & Dunne, K. A. (2016). Potential evapotranspiration and continental drying. *Nature Climate Change*, *6*, 946–949. https://doi.org/10.1038/nclimate3046

Mo, K. C., & Lettenmaier, D. P. (2016). Precipitation deficit flash droughts over the United States. *Journal of Hydrometeorology*, *17*(4), 1169–1184. Retrieved from https://journals.ametsoc.org/view/journals/hydr/17/4/jhm-d-15-0158_1.xml

Müller, W. A., Jungclaus, J. H., Mauritsen, T., Baehr, J., Bittner, M., Budich, R., et al. (2018). A higher-resolution version of the Max Planck Institute Earth System Model (MPI-ESM1.2-HR). *Journal of Advances in Modeling Earth Systems*, *10*(7), 1383–1413. https://doi.org/10.1029/2017MS001217

Novick, K. A., Ficklin, D. L., Stoy, P. C., Williams, C. A., Bohrer, G., Oishi, A. C., et al. (2016). The increasing importance of atmospheric demand for ecosystem water and carbon fluxes. *Nature Climate Change*, *6*(11), 1023–1027. https://doi.org/10.1038/nclimate3114

Null, S. E. (2016). Water supply reliability tradeoffs between removing reservoir storage and improving water conveyance in California. *JAWRA Journal of the American Water Resources Association*, *52*(2), 350–366. https://doi.org/10.1111/1752-1688.12391

Null, S. E., & Viers, J. H. (2013). In bad waters: Water year classification in nonstationary climates. *Water Resources Research*, *49*(2), 1137–1148. https://doi.org/10.1002/wrcr.20097

O'Gorman, P. A. (2015). Precipitation extremes under climate change. *Current Climate Change Reports*, *1*(2), 49–59. https://doi.org/10.1007/s40641-015-0009-3

Ohta, T., Maximov, T. C., Dolman, A. J., Nakai, T., van der Molen, M. K., Kononov, A. V., et al. (2008). Interannual variation of water balance and summer evapotranspiration in an eastern Siberian larch forest over a 7-year period (1998–2006). *Agricultural and Forest Meteorology*, *148*(12), 1941–1953. https://doi.org/10.1016/j.agrformet.2008.04.012

O'Neill, B. C., Tebaldi, C., van Vuuren, D. P., Eyring, V., Friedlingstein, P., Hurtt, G., et al. (2016). The Scenario Model Intercomparison Project (ScenarioMIP) for CMIP6. *Geoscientific Model Development*, *9*(9), 3461–3482. Retrieved from https://gmd.copernicus.org/articles/9/3461/2016/

Otkin, J. A., Svoboda, M., Hunt, E. D., Ford, T. W., Anderson, M. C., Hain, C., & Basara, J. B. (2018). Flash droughts: A review and assessment of the challenges imposed by rapid-onset droughts in the United States. *Bulletin of the American Meteorological Society*, *99*(5), 911–919. Retrieved from https://journals.ametsoc.org/view/journals/bams/99/5/bams-d-17-0149.1.xml

Palmer, M. A., Reidy Liermann, C. A., Nilsson, C., Flörke, M., Alcamo, J., Lake, P. S., & Bond, N. (2008). Climate change and the world's river basins: Anticipating management options. *Frontiers in Ecology and the Environment*, *6*(2), 81–89. https://doi.org/10.1890/060148

Pendergrass, A. G., & Knutti, R. (2018). The uneven nature of daily precipitation and its change. *Geophysical Research Letters*, *45*(21), 11980–11988. https://doi.org/10.1029/2018GL080298

Peng, L., Zeng, Z., Wei, Z., Chen, A., Wood, E. F., & Sheffield, J. (2019). Determinants of the ratio of actual to potential evapotranspiration. *Global Change Biology*, *25*(4), 1326–1343. https://doi.org/10.1111/gcb.14577

Polade, S. D., Pierce, D. W., Cayan, D. R., Gershunov, A., & Dettinger, M. D. (2014). The key role of dry days in changing regional climate and precipitation regimes. *Scientific Reports*, *4*(1), 4364. https://doi.org/10.1038/srep04364

Polson, D., Hegerl, G. C., Zhang, X., & Osborn, T. J. (2013). Causes of robust seasonal land precipitation changes. *Journal of Climate*, *26*(17), 6679–6697. Retrieved from https://journals.ametsoc.org/view/journals/clim/26/17/jcli-d-12-00474.1.xml

Post, A. K., & Knapp, A. K. (2020). The importance of extreme rainfall events and their timing in a semi-arid grassland. *Journal of Ecology*, *108*(6), 2431–2443. https://doi.org/10.1111/1365-2745.13478

Raymond, C., Horton, R. M., Zscheischler, J., Martius, O., AghaKouchak, A., Balch, J., et al. (2020). Understanding and managing connected extreme events. *Nature Climate Change*, *10*(7), 611–621. https://doi.org/10.1038/s41558-020-0790-4

Scanlon, B. R., Reedy, R. C., Faunt, C. C., Pool, D., & Uhlman, K. (2016). Enhancing drought resilience with conjunctive use and managed aquifer recharge in California and Arizona. *Environmental Research Letters*, *11*(3), 035013. https://doi.org/10.1088/1748-9326/11/3/035013

Scheff, J., Mankin, J. S., Coats, S., & Liu, H. (2021). CO2-plant effects do not account for the gap between dryness indices and projected dryness impacts in CMIP6 or CMIP5. *Environmental Research Letters*, *16*(3), 034018. https://doi.org/10.1088/1748-9326/abd8fd

Schewe, J., Heinke, J., Gerten, D., Haddeland, I., Arnell, N. W., Clark, D. B., et al. (2014). Multimodel assessment of water scarcity under climate change. *Proceedings of the National Academy of Sciences of the United States of America*, *111*(9), 3245–3250. Retrieved from https://www.pnas.org/content/pnas/111/9/3245.full.pdf

Seland, Ø., Bentsen, M., Olivié, D., Toniazzo, T., Gjermundsen, A., Graff, L. S., et al. (2020). Overview of the Norwegian Earth System Model (NorESM2) and key climate response of CMIP6 DECK, historical, and scenario simulations. *Geoscientific Model Development*, *13*(12), 6165–6200. Retrieved from https://gmd.copernicus.org/articles/13/6165/2020/

Siebert, S., Kummu, M., Porkka, M., Döll, P., Ramankutty, N., & Scanlon, B. R. (2015). A global data set of the extent of irrigated land from 1900 to 2005. *Hydrology and Earth System Sciences*, *19*(3), 1521–1545. Retrieved from https://hess.copernicus.org/articles/19/1521/2015/

Sims, C., & Null, S. E. (2019). Climate forecasts and flood mitigation. *Southern Economic Journal*, *85*(4), 1083–1107. https://doi.org/10.1002/soej.12331

Smerdon, B. D. (2017). A synopsis of climate change effects on groundwater recharge. *Journal of Hydrology*, *555*, 125–128. Retrieved from https://www.sciencedirect.com/science/article/pii/S0022169417306510

Smith, C. J., & Forster, P. M. (2021). Suppressed late-20th century warming in CMIP6 models explained by forcing and feedbacks. *Geophysical Research Letters*, *48*(19), e2021GL094948. https://doi.org/10.1029/2021gl094948

Swain, D. L., Langenbrunner, B., Neelin, J. D., & Hall, A. (2018). Increasing precipitation volatility in twenty-first-century California. *Nature Climate Change*, *8*(5), 427–433. https://doi.org/10.1038/s41558-018-0140-y

Swann, A. L. S., Hoffman, F. M., Koven, C. D., & Randerson, J. T. (2016). Plant responses to increasing CO2 reduce estimates of climate impacts on drought severity. *Proceedings of the National Academy of Sciences of the United States of America*, *113*(36), 10019–10024. https://www.pnas.org/content/pnas/113/36/10019.full.pdf

Swart, N. C., Cole, J. N. S., Kharin, V. V., Lazare, M., Scinocca, J. F., Gillett, N. P., et al. (2019). The Canadian Earth System Model version 5 (CanESM5.0.3). *Geoscientific Model Development*, *12*(11), 4823–4873. https://gmd.copernicus.org/articles/12/4823/2019/

Tebaldi, C., Debeire, K., Eyring, V., Fischer, E., Fyfe, J., Friedlingstein, P., et al. (2021). Climate model projections from the Scenario Model Intercomparison Project (ScenarioMIP) of CMIP6. *Earth System Dynamics*, *12*(1), 253–293. Retrieved from https://esd.copernicus.org/articles/12/253/2021/

Tichavský, R., Ballesteros-Cánovas, J. A., Šilhán, K., Tolasz, R., & Stoffel, M. (2019). Dry spells and extreme precipitation are the main trigger of landslides in Central Europe. *Scientific Reports*, *9*(1), 1–10.

Tokarska, K. B., Stolpe, M. B., Sippel, S., Fischer, E. M., Smith, C. J., Lehner, F., & Knutti, R. (2020). Past warming trend constrains future warming in CMIP6 models. *Science Advances*, *6*(12), eaaz9549. https://doi.org/10.1126/sciadv.aaz9549

Trenberth, K. E., Dai, A., Rasmussen, R. M., & Parsons, D. B. (2003). The changing character of precipitation. *Bulletin of the American Meteorological Society*, *84*(9), 1205–1218. https://doi.org/10.1175/bams-84-9-1205

Trugman, A. T., Anderegg, L. D. L., Shaw, J. D., & Anderegg, W. R. L. (2020). Trait velocities reveal that mortality has driven widespread coordinated shifts in forest hydraulic trait composition. *Proceedings of the National Academy of Sciences of the United States of America*, *117*(15), 8532–8538. Retrieved from https://www.pnas.org/content/pnas/117/15/8532.full.pdf

US Drought Monitor. (2021). Retrieved from https://droughtmonitor.unl.edu/

van Dijk, A. I. J. M., Beck, H. E., Crosbie, R. S., de Jeu, R. A. M., Liu, Y. Y., Podger, G. M., et al. (2013). The Millennium Drought in southeast Australia (2001–2009): Natural and human causes and implications for water resources, ecosystems, economy, and society. *Water Resources Research*, *49*(2), 1040–1057. https://doi.org/10.1002/wrcr.20123

Vicente-Serrano, S. M., Beguería, S., & López-Moreno, J. I. (2010). A multiscalar drought index sensitive to global warming: The standardized precipitation evapotranspiration index. *Journal of Climate*, *23*(7), 1696–1718. https://doi.org/10.1175/2009JCLI2909.1

Voldoire, A., Saint-Martin, D., Sénési, S., Decharme, B., Alias, A., Chevallier, M., et al. (2019). Evaluation of CMIP6 DECK experiments with CNRM-CM6-1. *Journal of Advances in Modeling Earth Systems*, *11*(7), 2177–2213. https://doi.org/10.1029/2019MS001683

Volodin, E., & Gritsun, A. (2018). Simulation of observed climate changes in 1850–2014 with climate model INM-CM5. *Earth System Dynamics*, *9*(4), 1235–1242. Retrieved from https://esd.copernicus.org/articles/9/1235/2018/

Wainwright, C. M., Black, E., & Allan, R. P. (2021). Future changes in wet and dry season characteristics in CMIP5 and CMIP6 simulations. *Journal of Hydrometeorology*, *22*(9), 2339–2357. https://doi.org/10.1175/jhm-d-21-0017.1

Wheater, H., & Evans, E. (2009). Land use, water management and future flood risk. *Land Use Policy*, *26*, S251–S264. Retrieved from https://www.sciencedirect.com/science/article/pii/S0264837709001082

Willis, A. D., Lund, J. R., Townsley, E. S., & Faber, B. A. (2011). Climate change and flood operations in the Sacramento Basin, California. *San Francisco Estuary and Watershed Science*, *9*(2). https://doi.org/10.15447/sfews.2011v9iss2art3

Wu, T., Lu, Y., Fang, Y., Xin, X., Li, L., Li, W., et al. (2019). The Beijing Climate Center Climate System Model (BCC-CSM): The main progress from CMIP5 to CMIP6. *Geoscientific Model Development*, *12*(4), 1573–1600. https://doi.org/10.5194/gmd-12-1573-2019

Yang, Y., Roderick, M. L., Zhang, S., McVicar, T. R., & Donohue, R. J. (2019). Hydrologic implications of vegetation response to elevated CO2 in climate projections. *Nature Climate Change*, *9*(1), 44–48. https://doi.org/10.1038/s41558-018-0361-0

Yin, Y., Byrne, B., Liu, J., Wennberg, P. O., Davis, K. J., Magney, T., et al. (2020). Cropland carbon uptake delayed and reduced by 2019 Midwest floods. *AGU Advances*, *1*(1), e2019AV000140. https://doi.org/10.1029/2019av000140

Yuan, W., Zheng, Y., Piao, S., Ciais, P., Lombardozzi, D., Wang, Y., & Yang, S. (2019). Increased atmospheric vapor pressure deficit reduces global vegetation growth. *Science Advances*, *5*(8), eaax1396. https://doi.org/10.1126/sciadv.aax1396

Yukimoto, S., Kawai, H., Koshiro, T., Oshima, N., Yoshida, K., Urakawa, S., et al. (2019). The Meteorological Research Institute Earth System Model Version 2.0, MRI-ESM2.0: Description and basic evaluation of the physical component. *Journal of the Meteorological Society of Japan Series II*, *97*(5), 931–965. https://doi.org/10.2151/jmsj.2019-051

Zhang, Y., Susan Moran, M., Nearing, M. A., Ponce Campos, G. E., Huete, A. R., Buda, A. R., et al. (2013). Extreme precipitation patterns and reductions of terrestrial ecosystem production across biomes. *Journal of Geophysical Research: Biogeosciences*, *118*(1), 148–157. https://doi.org/10.1029/2012jg002136

Zhou, S., Williams, A. P., Berg, A. M., Cook, B. I., Zhang, Y., Hagemann, S., et al. (2019). Land–atmosphere feedbacks exacerbate concurrent soil drought and atmospheric aridity. *Proceedings of the National Academy of Sciences of the United States of America*, *116*(38), 18848–18853. https://doi.org/10.1073/pnas.1904955116

Ziehn, T., Chamberlain, M. A., Law, R. M., Lenton, A., Bodman, R. W., & Dix, M. (2020). The Australian Earth System Model: ACCESS-ESM1.5. *Journal of Southern Hemisphere Earth Systems Science*, *70*(1), 193–214. Retrieved from https://www.publish.csiro.au/paper/ES19035

Zipper, S. C., Hammond, J. C., Shanafield, M., Zimmer, M., Datry, T., Jones, C. N., et al. (2021). Pervasive changes in stream intermittency across the United States. *Environmental Research Letters*, *16*(8), 084033. https://doi.org/10.1088/1748-9326/ac14ec